

ULTRACOMPACT OPTOFLEX NEURAL PROBES FOR HIGH-RESOLUTION ELECTROPHYSIOLOGY AND OPTOGENETIC STIMULATION

Maysamreza Chamanzar^{1*}, Daniel J. Denman², Timothy J. Blanche², and Michel M. Maharbiz¹

¹EECS Department, University of California Berkeley, Berkeley, USA

²Allen Institute for Brain Science, Seattle, USA

ABSTRACT

We report on the development of high-density neural probes for distributed neuronal recording and stimulation. Our hybrid silicon-parylene probes provide high spatial resolution and incorporate a monolithically integrated flexible cable to address the challenge of stable recordings in chronic neural implants. We address a long-standing but often overlooked issue in parylene processing to realize reliable multilayer interconnects. We also discuss the design of ultracompact parylene optical waveguides for localized optogenetic stimulation of neurons. We demonstrate in-vivo electrophysiology recordings in mice.

INTRODUCTION

Understanding the neural basis of brain function remains an elusive goal of systems neuroscience [1]. Existing neural probe technologies: lack the electrode array density necessary for reliably isolating action potentials (APs) from single neurons while also providing millimetric scale coverage of brain nuclei; are large and stiff which causes damage to the neuropil and vasculature; are prohibitively expensive, and are not scalable in a way that enables recordings from a large population of neurons in multiple adjacent brain areas. High-density silicon probes have been fabricated using electron beam lithography (EBL) [2], however EBL is a serial and low-throughput method that cannot be easily scaled up to mass-produce high-yield probes. Additionally, the rigid connection of probes to the recording circuitry is a contributing factor in the chronic inflammatory response that results in the formation of glial scarring and degradation of recording quality over time. To overcome this problem, polymer-based probes have been recently proposed [3]. The low stiffness of such probes makes implantation difficult and the density of recording channels is low because of the limited resolution of lithography on polymer substrates. To address these challenges, we have designed a process based on high-throughput deep UV (DUV) lithography to realize ultra compact implantable neural probes in a hybrid parylene-silicon platform [4]. Our neural probes thus inherit the benefits of both silicon-based and all-polymer neural implants.

Optogenetics is a powerful tool for perturbation of neural circuits [5] that would be even more powerful if light could be delivered locally to small subsets of neurons instead of illuminating whole brain regions using disruptive methods such as optical fibers. We performed quantitative modeling to show the possibility of realizing ultra compact all-parylene waveguides that can be monolithically integrated on the probe. We characterized the electrical properties of our probes and demonstrated their use in acute electrophysiology recordings in mice.

A schematic of our neural probe is shown in Figure 1. The probe shank is made of silicon with an insulating layer of parylene C and incorporates 64 recording sites. The shank is 20 μm thick, and 30-95 μm wide depending on the recording site configuration (which is usually the case for other probes where the shank width is determined by the size and number of interconnects). The 64 recording sites are routed through a high-density array of interconnects over the silicon shank, which are then connected monolithically to the corresponding array of interconnects embedded in a thin (8 μm) parylene C ribbon cable. This compliant cable conducts the recorded signals through the skull to the head-mounted recording electronics. The flexible nature of this cable allows the implanted probes to ‘float in the brain’ and move coherently with the brain micromotion, thus minimizing the tethering force on the brain tissue. The end of the parylene cable is also monolithically connected to a stiff silicon backend, where the traces expand and end in an array of bond pads on silicon to allow integration with the recording circuitry possible using standard packaging methods such as wire- or flip-chip bonding.

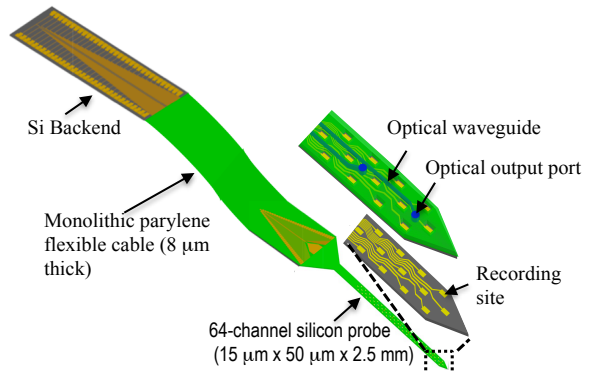


Figure 1: Schematic of the hybrid silicon-parylene probe

FABRICATION PROCESS

To realize high-yield and compact neural probes, we designed a fabrication process in which the silicon layer and the parylene layers are realized in different steps on the same wafer. We optimized the process so that more than 500 probes can be made on a 6-inch wafer. A simplified version of the fabrication process highlighting the important steps is shown in Figure 2. First, we grow thermal oxide at 1000C in a Tystar furnace to a thickness of 1 μm on a SOI wafer with a device layer of 15 μm that defines the thickness of the probe shank and the backend. Then, using a DUV ASML5500/300 stepper, we define the recording sites and the high resolution interconnects. A stack of Ti/Au/Pt with thicknesses of

100A/1400A/100A is deposited using a CHA evaporation system. Ti provides good adhesion to the oxide layer and Pt is used to ensure a strong adhesion to parylene. Following a lift off process, the recording sites and interconnects are realized. We optimized the process to realize \sim 250 nm space and trace interconnects along the 2 mm length of the probe shank with a near perfect yield (Figure 3). In the next step, parylene is conformally deposited to a thickness of 4 μm in a SCS Labcoater 2010 machine. A-174 silane in vapor phase is used to enhance the adhesion of parylene to the underlying layer. Next, vias are etched in parylene using an oxygen plasma process to connect the first layer interconnects to the cable tracks, subsequently defined using another lithography and lift off process. This way the interconnects on SiO_2 layer are routed on top of the parylene layer through etched vias.

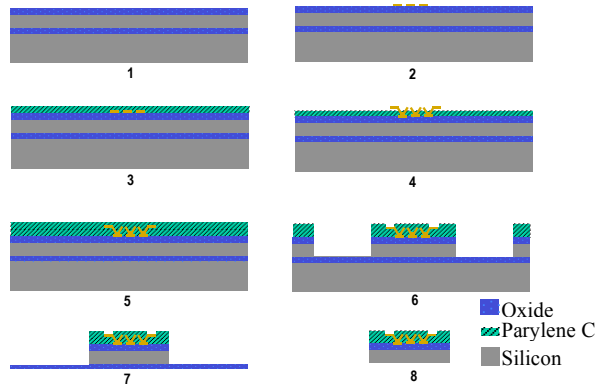


Figure 2: The fabrication process starts with patterning the first layer interconnects on an SOI wafer, followed by parylene C deposition and a second layer of interconnects on parylene C. Then the recording sites are etched and exposed; the probe outline is defined and etched; and finally the probes are released.

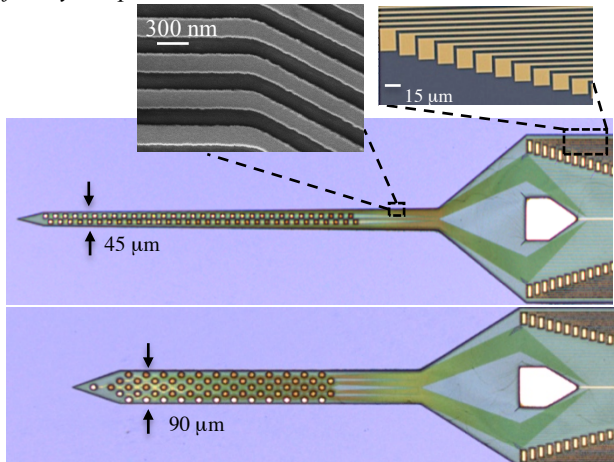


Figure 3: Optical micrographs of two different probe shanks. Left inset shows a scanning electron micrograph of interconnects on the shank. Right inset shows 4 μm tacks at the silicon-parylene cable interface.

Another layer of parylene is deposited to a thickness of 4 μm to completely embed interconnects in parylene thus forming the cable. The resulting cable is only 8 μm thick and extremely compliant (with the cantilever stiffness of $k_{\text{cant}} \sim 10^{-5}$ N/m). In the next step, the outlines of the

devices are etched in parylene, oxide, and silicon layers. The wafer is mounted on a carrier wafer to release the devices from the backside in parallel. This process is high throughput. Based on probe station tests on a few different wafers, more than 90% of the devices on the wafer were functional, with some devices close to the rim partially damaged mostly due to etching non-uniformities.

PARYLENE INTERCONNECT PROCESS CONSIDERATIONS

Parylene C has been widely used as a highly inert and biocompatible material in a range of implantable devices. To realize functional devices, parylene needs to be patterned, etched, and integrated with other materials. Despite the favorable properties of parylene films, processed parylene-based devices suffer from stability and longevity issues, especially when implanted in the body. We have identified two main causes that potentially contribute to the failure of parylene devices. One problem is the residue that remains on vias after plasma etching of parylene. This microstructured residue (shown in Figure 4a) is extremely difficult to remove, even after extensive overetching using oxygen plasma. The poor electrical connection and a high chance of delamination result in a very unstable layer-to-layer connection. To solve this issue, we have designed a process based on an aluminum sacrificial etch stop layer to lift off the remnant residue. The second problem is the very poor quality worm-holed sidewalls when etching parylene using standard oxygen plasma recipes (Figure 4a). Over-etching damages sidewalls by aggressively undercutting while leaving behind worm-holed walls, which are hard to see without SEM imaging. These porous etched sidewalls allow for permeation of liquid, proteins and other molecules and therefore failure and delamination of the patterned and etched parylene layers. We have optimized a custom DRIE recipe consisting of alternating O_2 plasma (600W, 60 mTorr)/ fluoropolymer deposition steps (6 sec / 7 sec) to achieve smooth and seamless sidewalls (Fig. 4b).

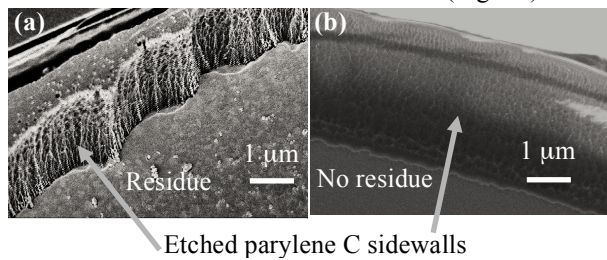


Figure 4: (a) A via etched in Parylene C using anisotropic O_2 plasma etching (200W, 80 mTorr), where rough sidewalls and residues at the bottom are evident. (b) the same structure etched using our DRIE recipe with alternate C_4F_8 deposition and O_2 plasma etching and an Al sacrificial etch stop layer. The sidewalls are smooth and no residue is left at the bottom.

We verified the reliability of the vertical metal interconnects through different layers of parylene C after these process innovations. Probe station tests on three different wafers revealed that the yield of the interconnections at the junction of the cable and the probe shank were increased from 30% to more than 96% after we optimized the parylene etching process. Moreover, we

tested the mechanical stability of the released probes in Phosphate Buffered Saline (PBS 1X) for 8-hour periods over 30 days. No degradation of impedance was observed. In addition, we measured the impedance spectrum before and after several implantations, where again the electrical impedances of the channels remained stable. These observations further corroborate the importance of having high-quality etched layers in parylene C to enhance the mechanical stability and prevent failures *in vivo*.

FLEXIBLE OPTICAL WAVEGUIDES FOR LOCAL OPTOGENETIC STIMULATION

Despite recent advances in neural modulation techniques, including a rapidly expanding optogenetic toolset [5, 6], still we lack a robust, minimally-invasive optogenetic stimulation platform [6]. The ability to independently deliver light to multiple, highly localized ($\sim 50 \mu\text{m}^3$) subsets of neurons that are simultaneously recorded on the electrode array would drastically improve the sensitivity and interpretability of *in vivo* optogenetic experiments. Illuminating a large volume of neuropil using light sources on the surface of the brain does not provide the requisite spatial resolution and since the intensity falls off rapidly, only a small fraction of target neurons in the vicinity of the light source ($\sim 200 \mu\text{m}$) will be excited. Increasing the light source power, on the other hand, results in the generation of excessive heat in the brain and the potential for phototoxicity [7]. Given a scattering coefficient of 11 mm^{-1} in the mouse brain and the minimum threshold intensity of 1 mW/mm^2 for a channelrhodopsin to evoke action potentials [8], an input power of 2.25 mW is required in a fiber optic ($200 \mu\text{m}$, NA=0.37) to excite a neuron at a depth of 2 mm into the cortex resulting in a (very high) intensity of 71.6 mW/mm^2 at the output aperture of the fiber, sufficient to cause damage to the brain tissue. This trade-off between the range of stimulation and the required optical power results in an inherently low spatial resolution. To reach deeper brain regions, bare fibers (typically $100\text{--}200 \mu\text{m}$ in diameter) are inserted, causing a large tissue displacement and introducing a tethering force on the brain. Recently, photonic waveguide devices have been used to deliver light locally deep into the brain [7, 10]. These implementations are based on semiconductor and dielectric materials such as SiO₂ and Oxynitride [7, 10]. Such waveguides, although compact, are stiff and cannot be integrated with a neural implant such as the one we have introduced in this paper with both stiff and flexible parts. Material biocompatibility and mechanical stability is always a point of concern, especially for chronic implants.

Here we introduce a novel integrated photonic device platform to realize ultra-compact all-parylene photonic waveguides. Parylene waveguides are flexible, and can be monolithically integrated with the insulating parylene C layer to deliver light from outside the brain to specific locations along the probe shank. The core of the waveguide is made of parylene N, which has a higher refractive index than the parylene C cladding layer. The parylene C cladding serves as an intermediate layer between the electrical layer of the probe and the optical layer (Figure 1). Ellipsometry of the parylene films

revealed a refractive index of 1.66 for parylene C and 1.786 for parylene N at the wavelength of $\lambda = 480 \text{ nm}$, which is the excitation wavelength for channelrhodopsins. The fabrication process consists of implementing trenches in parylene C and depositing parylene N to form ridge waveguides. An etchback step is used to remove the rib layer that forms in between the waveguides as a result of the conformal deposition of parylene N. Finally, the waveguide array is encapsulated in a cladding layer of Parylene C. An array of fabricated optical waveguides on a stand-alone parylene substrate is shown in Figure 5a. Finite Element simulations show that a very compact waveguide with a cross section of $3 \mu\text{m} \times 3 \mu\text{m}$ can support a confined guided mode at the wavelength of $\lambda = 480 \text{ nm}$ (Figure 5b). This novel integrated photonic material consisting of only parylene layers is seamless, biocompatible, and compliant. We believe such a parylene-in-parylene (PiP) integrated photonic device platform can find interesting applications for a new class of implantable integrated photonic devices, beyond neural probes, where different functional devices such as waveguides, resonators, and filters can be easily implemented.

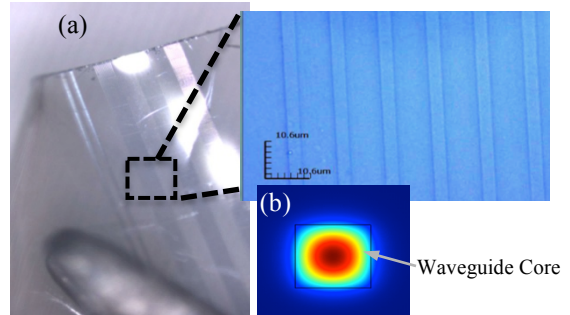


Figure 5: (a) optical micrograph of an array of optical waveguides on a parylene film. (b) The field profile of the confined optical mode of a $3 \mu\text{m} \times 3 \mu\text{m}$ waveguide.

ELECTRICAL CHARACTERIZATION

After the probes are released from the wafer, we package them with a custom-designed adaptor PCB that connects the probe to the headstage recording circuitry (e-cube, White Matter LLC). We designed a die-attach robot capable of finding and assembling released probes from a tray. A fine pitch wire bonder was used to wirebond the probe to the PCB. A packaged probe is shown in Figure 6.

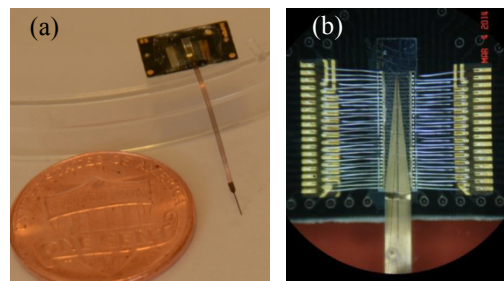


Figure 6: (a) Our 64-channel hybrid parylene-silicon probe, consisting of a high-density silicon shank ($50 \mu\text{m} \times 15 \mu\text{m} \times 2 \text{ mm}$) and a flexible parylene cable ($8 \mu\text{m} \times 500 \mu\text{m} \times 20 \text{ mm}$) assembled to the headstage adaptor PCB. (b) Backend wirebonded with the adaptor PCB.

We characterized the electrical properties of the probes by measuring the recording site impedances in Phosphate Buffered Solution (PBS 1X) using a nanoZ impedance spectrum analyzer (White Matter LLC). To improve the signal-to-noise-ratio (SNR), conductive polymer Poly(3,4-ethylenedioxythiophene) Polystyrene sulfonate (PEDOT:PSS) was electroplated on the recording sites. The impedance spectra of a typical recording site is plotted in Figure 7, before and after electroplating with a 0.2 M concentration of PEDOT:PSS and a total charge deposition of 6 μ C. The impedance was reduced by an order of magnitude. Since the recording sites are recessed in parylene, the parylene sidewalls prevent enlargement of the sites, which prevents possible shorting with other sites during plating. PEDOT-filled recording sites have a lower noise floor without increase in the electrode cross-sectional area, which effectively increases the SNR of extracellular neural recordings.

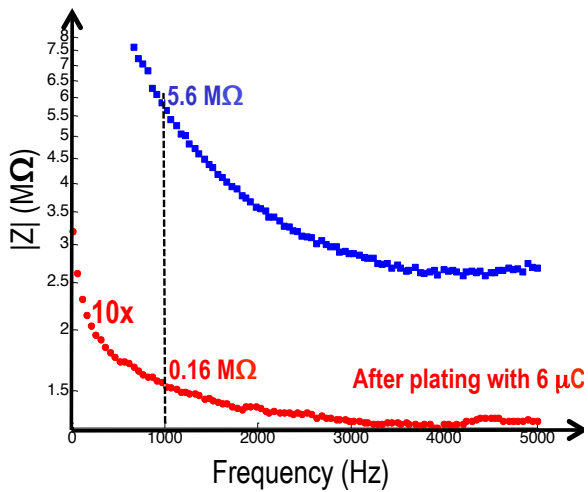


Figure 7: The impedance spectra for a $\sim 113\mu\text{m}^2$ recording site before (blue) and after (red) electroplating in PEDOT:PSS. The spectrum after electroplating is plotted with 10x amplification for legibility.

Another advantage of recessed recording sites is the stability of the electroplated PEDOT layer in the brain. As can be seen in Figure 8, the deposited PEDOT polymer layer is protected by the parylene sidewalls and does not easily come off during implantation. We performed repeated insertion tests that showed that the impedances of the sites are stable with multiple insertions in the brain.

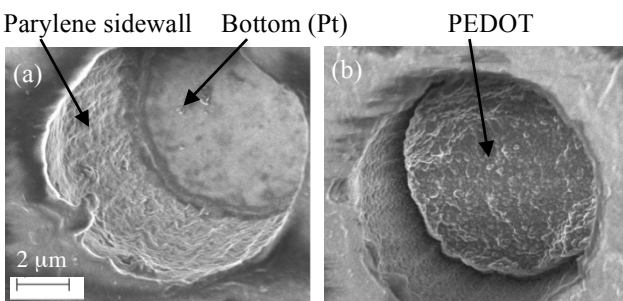


Figure 8: (a) The native Pt recording site at the bottom of a parylene hole. (b) Electroplated PEDOT conductive polymer on the recording site.

IN-VIVO TESTS

We implanted our neural probes in the visual cortex of wildtype (C57) mice using a robotic stereotaxic micro-manipulator (Neurostar, Germany) equipped with piezo microtweezers (Figure 9a). Acute in-vivo recordings with excellent SNR were demonstrated (Figure 9b).

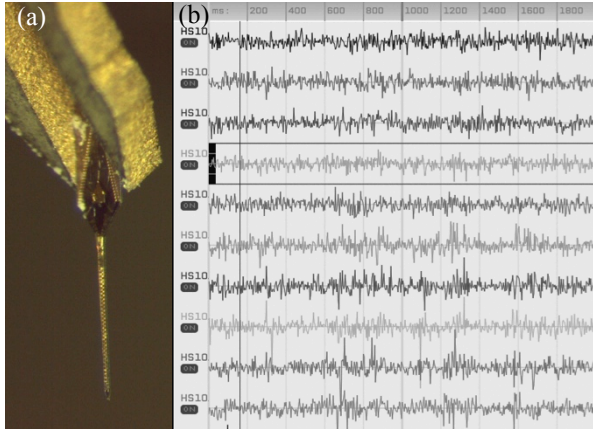


Figure 9: (a) a probe held by piezo microgrippers above the cortex prior to implantation. (b) acute extracellular recordings of ten representative channels, high-pass filtered (300-6kHz) to show neural action potentials.

ACKNOWLEDGEMENTS

This project was supported by the National Science Foundation, IDBR grant # 1152658.

REFERENCES

- [1] G. Buzsaki, *Nature Neuroscience* vol. 7, p. 446, 2004.
- [2] J. Du, T. J. Blanche, R. R. Harrison, H. A. Lester, and S. C. Masmanidis, *PLoS One*, vol. 6, p. e26204, 2011.
- [3] J. P. Seymour, D. R. Kipke, *Engineering in Medicine and Biology Society*, 2006. EMBS '06, p. 4606, 2006.
- [4] C. Pang; J.G. Cham, Z. Nenadic, S. Musallam, Y. Tai; J. W. Burdick, R. A. Andersen, *Engineering in Medicine and Biology Society*, 2005. EMBS '05, p. 7114, 2005.
- [5] L. Fenno, O. Yizhar, K. Deisseroth, *Annual review of neuroscience*, vol. 34, p. 389, 2011.
- [6] E. S. Boyden, *F1000 Biology reports* 2011.
- [7] A. N. Zorzos, J. Scholvin, E. S. Boyden, *Optics letters*, vol. 37, p. 4841, 2012.
- [8] O. Yizhar, L. E. Fenno, T. J. Davidson, M. Mogri, K. Deisseroth, *Neuron*, vol. 71, p. 9, 2011.
- [9] A. M. Aravanis, L. P. Wang, F. Zhang, L. Meltzer, M. Mogri, M. B. Schneider, K. Deisseroth, *Journal of neural engineering*, vol. 4, p. S143, 2007.
- [10] T. V. Abaya, S. Blair, P. Tathireddy, L. Rieth, F. A. Solzbacher, *Biomedical optics express*, vol. 3, p. 3087, 2012.

CONTACT

*M. Chamanzar, chamanzar@berkeley.edu